DEFECT BEHAVIOR IN ELECTRON-IRRADIATED BORON- AND GALLIUM-DOPED SILICON

Peter J. Drevinsky and Henry M. DeAngelis
Rome Air Development Center
Hanscom Air Force Base, Massachusets

ABSTRACT

Production and anneal of defects in electron-irradiated, float-zone silicon solar cells were studied by DLTS. In boron- and gallium-doped, n^+-p cells, dominant defects were due to the divacancy, carbon interstitial, and carbon complex. Results suggest that the DLTS peak normally ascribed to carbon complexes also involves gallium. For gallium- and, to a lesser extent, boron-doped samples, damaged lifetime shows substantial recovery only when the carbon-complex peak has annealed out at 400°C. In boron-doped, n^+-p-p^+ cells, a minority carrier trap (E1) was also observed by DLTS in cells with a boron p^+, but not in those with an aluminum p^+ back. A level at E_V + 0.31 eV appeared upon 150°C annealing (E1 out) in both p^+ back types of samples.

INTRODUCTION

In electron-irradiated electronic devices such as solar cells, interactions between dopant, intrinsic impurities, and point defects can lead to the formation of damaging complexes. Irradiation of boron-doped silicon, for example, can produce various defects involving boron, carbon, oxygen, vacancies, and interstitials. Techniques such as Deep Level Transient Spectroscopy (DLTS) have been used (refs. 1 to 3) for defect detection. Weinberg and Swarz (refs. 4 and 5), in correlating the annealing behavior of defects observed by DLTS (ref. 3) with short circuit current (J_{SC}), attributed the observed reverse anneal of J_{SC} to the emergence of the E_V + 0.30 eV level. Rohatgi (ref. 6) also concluded from DLTS measurements that this defect is responsible for reverse annealing in irradiated boron-doped cells.

This report describes results of our DLTS studies of defects in electron-irradiated solar cells fabricated from float-zone silicon. Since irradiated gallium-doped cells have shown a potential for greater recovery after anneal than boron-doped cells (ref. 7), we have compared radiation-induced defects in high purity, n^+-p silicon cells doped with gallium and boron. Results of defect annealing studies are presented and minority carrier lifetime measurements are correlated with defect anneal. Defect production and annealing behavior have also been studied in a set of boron-doped, n^+-p-p^+ silicon cells, which were fabricated with either an aluminum p^+ or a boron p^+ back surface.

EXPERIMENTAL

Diffused junction, n^+-p cells, doped with either gallium (2, 10, and 20 ohm-cm) or with boron (2 ohm-cm), were fabricated by Spectrolab, Inc. from high purity, float-zone silicon (ref. 8). A second set consisted of diffused junction, n^+-p-p^+ cells doped with boron (1 and 10 ohm-cm) and fabricated by Comsat Laboratories from float-zone silicon. Cells for each base resistivity had an aluminum and boron p^+ back surface and these will be referred to as Al p^+ and B p^+, respectively. Processing conditions were: All Al p^+ cells - no pre-oxidation, single-step phosphorus front and aluminum back diffusion at 850°C for 30 min., and no post, or final, anneal; 10 ohm-cm, B p^+ cells - no pre-oxidation, boron back diffusion at 950°C for 30 min., phosphorus front diffusion at 850°C for 15 min., and post anneal at 450°C for 14 hrs.; 1 ohm-cm, B p^+ cells - identical to the 10 ohm-cm, B p^+ cells except for pre-oxidation at 1050°C for 30 min. Cells were diced into chips 0.25 cm on edge and these were mesa-etched to minimize leakage current, mounted on TO-5 headers with silver epoxy, and top-contacted by ultrasonic bonding (refs. 9 and 10).

Defects were detected by DLTS (ref. 11) by using the lock-in amplifier version of the technique (ref. 12). For bias pulse voltages and base resistivities used, the regions approximately 0.3 to 3 micrometers below the metallurgical junction could be examined. Minority carrier lifetime was measured by a diode reverse recovery technique and deeper levels unobservable by DLTS were monitored by capacitance-voltage measurements. Short circuit current was measured on either 1x1 cm or 1x2 cm cell pieces with the use of a Spectrolab solar simulator.

Samples were irradiated in air at room temperature with 1-MeV electrons to fluences ranging from $1.0\text{x}10^{15}$ to $1.6\text{x}10^{16}$ e^-/cm^2, measured within one day after irradiation, and stored in dry ice. Lower fluences were used on cells and on companion samples for accompanying DLTS scans and minority carrier lifetime measurements. Samples were isochronally annealed to 100°C in air and continued to about 425°C in a nitrogen atmosphere for periods of either 20 or 30 minutes at temperature.

RESULTS AND DISCUSSION

Principal DLTS peaks in irradiated samples were found to be majority carrier traps associated with levels at E_V + 0.21eV (H1, divacancy), +0.27ev (H2, carbon interstitial), and +0.34eV (H3, carbon complex). A minority carrier trap at E_V-0.26eV (E1, boron complex) was observed for boron-doped, B p^+ samples and upon annealing at 150°C, this level disappeared and another majority carrier trap at E_V + 0.31eV (H4) emerged.

n^+-p cells

Figure 1 shows DLTS spectra of 2, 10 and 20 ohm-cm ($6.5\text{x}10^{15}$, $1.4\text{x}10^{15}$, and $5.9\text{x}10^{14}$ cm^{-3}, respectively), gallium-doped silicon samples irradiated to a fluence of $5\text{x}10^{15}e^-/cm^2$. The three dominant majority carrier traps H1, H2, and H3 are attributed to the divacancy (ref. 2), carbon interstitial (ref. 2), and carbon

complexes, respectively. The identity of these carbon complexes is uncertain and they have been described as a carbon interstitial-substitutional pair (C_I-C_S) in reference 2 and as a vacancy-oxygen-carbon complex (V-O-C) in reference 3. It is apparent that the amplitude of H3 is gallium concentration dependent, increasing as the gallium content increases. It is interesting to note that the relative concentrations of H2 to H3 decrease with increasing gallium concentration. The introduction rate for H1 is essentially constant for all three sample resistivities. It should be noted that boron-doped samples showed H1 and H2, but little or no production of H3.

Isochronal anneals from 50° to 100°C indicate that the gallium content apparently influences the anneal of the carbon interstitial, which disappeared more rapidly in the order of decreasing resistivity. We have not observed similar behavior in float-zone, boron-doped silicon. Peak H3 grew during this annealing sequence, and the largest increase occurred in the 20 ohm-cm samples.

The most dramatic example of the effect of gallium on annealing behavior is given in figure 2 which shows the anneal of peak H3. The annealing data were normalized to the amplitude of peak H3 after the 100°C annealing step. It is clearly seen that peak H3 involved at least two defects as an annealing stage centered at about 175°C appears and becomes more pronounced with increasing gallium concentration. Peak H3 may contain a carbon complex, but it also contains another defect which involves gallium in some way. Continuing the anneal, one finds a significant growth in peak H3, again showing a greater fractional growth for the lower gallium concentration. Note that this behavior was observed in other gallium-doped float-zone as well as crucible-grown, samples separately prepared from 1 and 10 ohm-cm silicon wafers. A detailed analysis of peak H3 at the 100°C step, at and after the 175°C annealing stage, and at the maximum growth point of 300°C has not yet been done. Essentially complete recovery is achieved after the 400°C anneal. The divacancy annealed out at 250°C to 300°C. It should be noted that an unidentified majority carrier trap, shallower than H3, emerged during the anneal at about 200°C and disappeared after the 400°C step.

Degradation and recovery of minority carrier lifetime was followed after each irradiation and annealing step for all gallium-doped samples. The data for 20 ohm-cm samples are shown in figure 3 which depicts the annealing behavior of peak H3, the lifetime, and the recovery of "deeper levels" not observable by DLTS but monitored by capacitance-voltage measurements. It is noted that the substantial growth in peak H3 coincides with the complete anneal of the deeper levels. Lifetime shows no significant recovery until H3 has annealed out at the 400°C step at which point it recovered to about 60 percent of its pre-irradiation value. The recovery of lifetime in the 2 and 10 ohm-cm, gallium-doped samples followed a similar pattern.

Figure 4 shows defect annealing data and lifetime measurements as a result of isochronal anneals from 50°C to 400°C for the 2 ohm-cm, boron-doped silicon. The anneal of peak H2, attributed primarily to the carbon interstitial, is essentially complete by about 75°C. No explanation for the residual which persists at 100°C can be given at this time. The growth of H3 is evident, but not significant until one exceeds 225°C. No secondary annealing stage appears as in gallium-doped samples. Peak H3 reaches a maximum at 350°C and anneals out by 400°C. The peak H4 was first observed after the 150°C anneal and it has been suggested that it is either a boron-oxygen-vacancy (B-O-V) in reference 3 or a silicon interstitial pair (Si_I-Si_I) in reference 2. It continues to grow, peaks at 350°C, and anneals out at 400°C. Annealing behavior was found to be similar in crucible-grown, boron-doped silicon.

It is important to note that lifetime does not recover until the 400°C anneal step at which point H3 and H4 are gone and even then only to about 20 percent of the pre-irradiation values. Our lifetime measurements on these boron-doped samples give no suggestion of a reverse anneal.

n^+-p-p^+ cells

Figure 5 shows typical DLTS spectra, taken under injection conditions, of 10 ohm-cm, boron-doped, Al p^+ and B p^+ samples irradiated to a fluence of $1x10^{15}$ e^-/cm^2. The most striking difference is the presence of a minority carrier trap (E1) in B p^+ and its absence in Al p^+ samples. It is important to note that DLTS samples of both types of cells were well-behaved diodes with similar dark current-voltage and injection characteristics. Also, cells had been prepared from the same silicon ingot. In spite of being identical samples, except for back surface type and processing, only B p^+ showed E1. Figure 5 also shows evidence for peak H3 in both sample types, quite suppressed in Al p^+. Peaks H1 and H2 appear in comparable quantities in both types.

The absence of a distinct reverse anneal in irradiated, high-purity, boron-doped silicon (see fig. 4) as followed by lifetime measurements with the diode reverse recovery technique led to a study of cell annealing behavior. Companion 10 ohm-cm cells and DLTS samples were irradiated simultaneously. Figure 6 shows the isochronal anneal, using J_{SC} measurements, of four types of cells including a 10 ohm-cm, gallium-doped cell for comparison. It is clear that the Al p^+ and B p^+ cells show similar trends and recovery characteristics, with a reverse anneal in the 200° to 300°C region and virtually complete recovery after annealing at 400°C. The 2 ohm-cm crucible-grown cell behaves similarly. The gallium-doped cell does not show the pronounced reverse anneal and, in fact, recovers in the 200° to 300°C region. Generally, this annealing behavior is similar to that reported earlier (ref. 13) in an extensive study of annealing performance of solar cells. Companion DLTS samples showed spectra similar to those presented in figure 7 and defect annealing behavior similar to that shown in figure 8. Although these figures show data for more heavily-irradiated samples, they demonstrate that deeper levels, H3, and H4 are present in significant concentrations during the reverse anneal experienced by the boron-doped cells.

In figure 7, typical DLTS spectra for 10 ohm-cm, B p^+ samples after irradiation to a fluence of $1.6x10^{16}e^-/cm^2$ and after three representative annealing steps are shown. Al p^+ samples gave similar spectra, except for the absence of E1. The fractional original minority carrier lifetime (τ/τ_0) is given in parentheses under the irradiation fluence and the annealing temperature. Note that the spectrum after the 427°C anneal was taken at ten times greater sensitivity than that for the other three spectra. Each given peak is labeled once as it first appears. The prominent peaks observed after irradiation are identical to those obtained for the more lightly-irradiated B p^+ shown in figure 5. When these anneal out, a new generation of defects appears in lower concentration. At 177°C, H2 is gone, H3 has grown, and H4 has come in at a temperature associated with the disappearance of E1. H1 is still present in its post-irradiation concentration. At 355°C lifetime begins to show recovery and it is important to note that capacitance-voltage measurements show that deeper levels have now annealed out. The spectrum shows a loss in H3 and the appearance of small quantities of unidentified defects, H5 and H6. At 427°C, the spectrum at greater sensitivity shows the loss

of essentially all of the initial radiation-produced defects and the presence of additional, unidentified H7, H8, and H9 defects. Lifetime has begun to show substantial recovery in this boron-doped sample. Other boron-doped samples have shown as much as 30 percent recovery at this temperature.

Figure 8 shows the annealing behavior of defects introduced by irradiating 10 ohm-cm, B p^+ samples to a fluence of 1.6×10^{16} e^-/cm^2. Except for the absence of E1 and smaller production of H3, defects in 10 ohm-cm, Al p^+ samples showed similar annealing behavior for this fluence. The total radiation-induced defect concentration for each p^+ type is nearly the same and estimated to be about 4×10^{14} cm^{-3} for these samples.

CONCLUDING REMARKS

We have observed significant differences in the defect production and annealing behavior of float-zone silicon, comparably doped with gallium and boron. The recovery of J_{SC} in limited annealing studies of gallium- and boron-doped silicon solar cells reflects some of these differences.

In n^+-p-p^+ samples, a minority carrier trap located at E_c - 0.26eV was observed in those with a B p^+ back, but not observed in those with an Al p^+ back surface. The differences in processing of these cells does introduce oxygen into the B p^+ cells. There may be sufficient oxygen in these samples to produce the B_I-O_I complex suggested in reference 3. We clearly observed the minority carrier trap in crucible-grown silicon, comparably doped with boron. Regardless of whether we observe the minority carrier trap or not in n^+-p-p^+ samples, E_v + 0.31eV grows in. Both B p^+ and Al p^+ show the influence of this growth in the reverse anneal.

Additional study is needed on diodes fabricated from float-zone, boron-doped silicon which is of high purity and low carbon content. Diodes should be fabricated such that oxygen is not introduced in processing or introduced in a carefully controlled manner.

REFERENCES

1. Lang, D. V.: Deep-Level Transient Spectroscopy: A New Method to Characterize Traps in Semiconductors. J. Appl. Phys., Vol. 45, no. 7, July 1974, pp. 3023-3032.

2. Kimerling, L. C.: Defect States in Electron-Bombarded Silicon: Capacitance Transient Analysis. Radiation Effects in Semiconductors, N. B. Urli and J. W. Corbett, eds., Institute of Physics Conference Series No. 31, Institute of Physics (London), 1977, pp. 221-230.

3. Mooney, P. M.; Cheng, L. J.; Suli, M.; Gerson, J. D.; and Corbett, J. W.: Defect Energy Levels in Boron-Doped Silicon Irradiated with 1-MeV Electrons. Phys. Rev. B, vol. 15, no. 8, Apr 15, 1977, pp. 3836-3843.

4. Weinberg, I.; and Swarz, C. K.: Reverse Annealing in Radiation-Damaged, Silicon Solar Cells. NASA Conference Publication 2097, 1979, pp 161-171.

5. Weinberg, I.; and Swartz, C. K.: Origin of Reverse Annealing in Radiation-Damaged Silicon Solar Cells. Appl. Phys. Lett., vol. 36, no. 8, Apr. 15, 1980, pp. 693-695.

6. Rohatgi, A.: Radiation Tolerance of Boron Doped Dendritic Web Silicon Solar Cells. NASA Conference Publication 2169, 1980, pp. 281-288.

7. Rahilly, W. P.; Scott-Monck, J.; Anspaugh, B.; and Locker, D.: Electron and Photon Degradation in Aluminum, Gallium and Boron Doped Float Zone Silicon Solar Cells. Twelfth Photovoltaic Specialists Conference - 1976, IEEE, 1976, pp. 276-281.

8. Fodor, J.; and Opjorden, R.: Advanced Silicon Materials for Space Solar Cells. Fourteenth Photovoltaic Specialists Conference - 1980, IEEE, 1980, pp. 882-886.

9. Drevinsky, P. J.; Schott, J. T.; DeAngelis, H. M.; Kirkpatrick, A. R.; and Minnucci, J. A.: Detection of Processing- and Radiation-Induced Defects in Solar Cells by Transient Capacitance Spectroscopy. Thirteenth Photovoltaic Specialists Conference - 1978, IEEE, 1978, pp. 1232-1237.

10. Drevinsky, P. J.; DeAngelis, H. M.; Schott, J. T.; and Rahilly, W. P.: DLTS Spectra and Defect Effects on Irradiated Silicon Solar Cells. Fourteenth Photovoltaic Specialists Conference - 1980, IEEE, 1980, pp. 835-839.

11. Miller, G. L.; Lang, D. V.; and Kimerling, L. C.: Capacitance Transient Spectroscopy. Ann. Rev. Mater. Sci., vol. 7, Annual Reviews, Inc., 1977, pp. 377-448.

12. Schott, J. T.; DeAngelis, H. M.; and Drevinsky, P. J.: Capacitance Transient Spectra of Processing- and Radiation-Induced Defects in Silicon Solar Cells. J. Elec. Mater., vol. 9, no. 2, 1980, pp. 419-434.

13. Scott-Monck, J. A.; and Anspaugh, B. E.: Effects of Dopants on Annealing Performance of Silicon Solar Cells. NASA Conference Publication 2097, 1979, pp. 173-183.

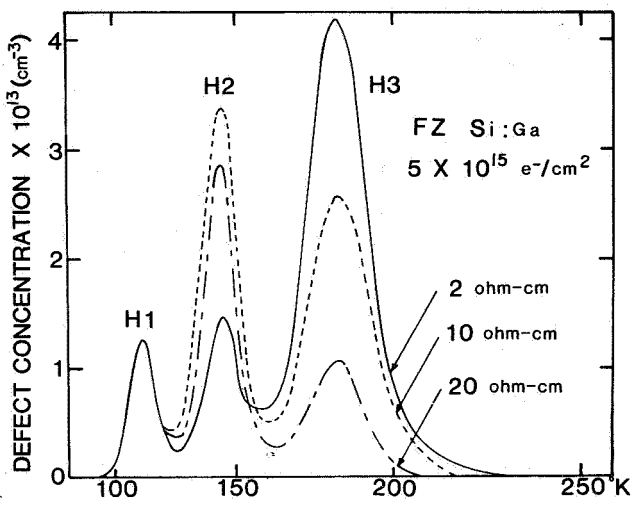

Figure 1. DLTS spectra of 1-MeV electron-irradiated, float zone silicon at various gallium doping levels.

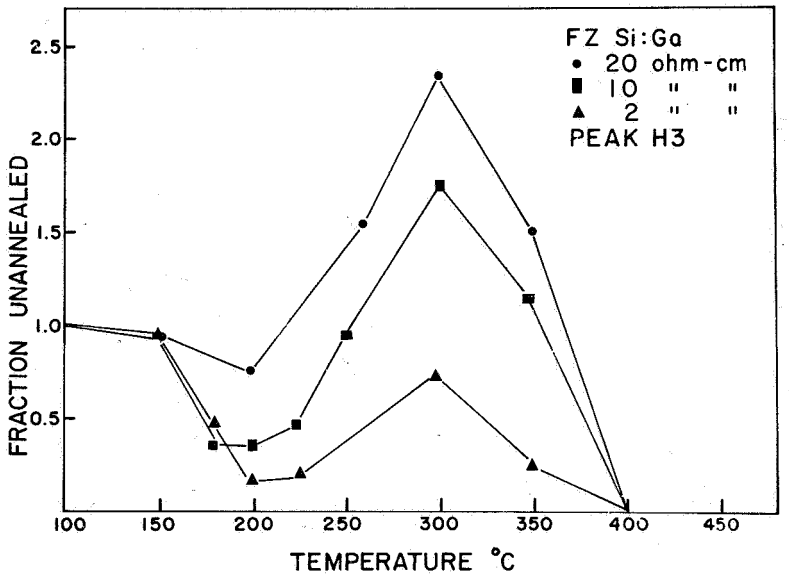

Figure 2. Isochronal anneal of the carbon-related peak (H3) in gallium-doped silicon irradiated with 1-MeV electrons ($5x10^{15}$ e^-/cm^2).

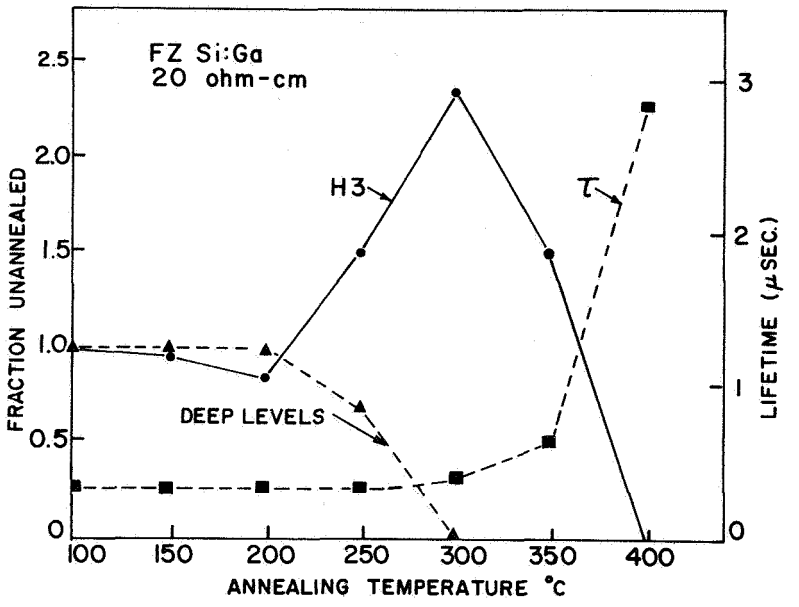

Figure 3. Isochronal anneal of the carbon-related peak (H3) in 1-MeV electron irradiated ($5x10^{15}$ e^-/cm^2) 20 ohm-cm, gallium-doped silicon as well as anneal of deep levels and recovery of lifetime.

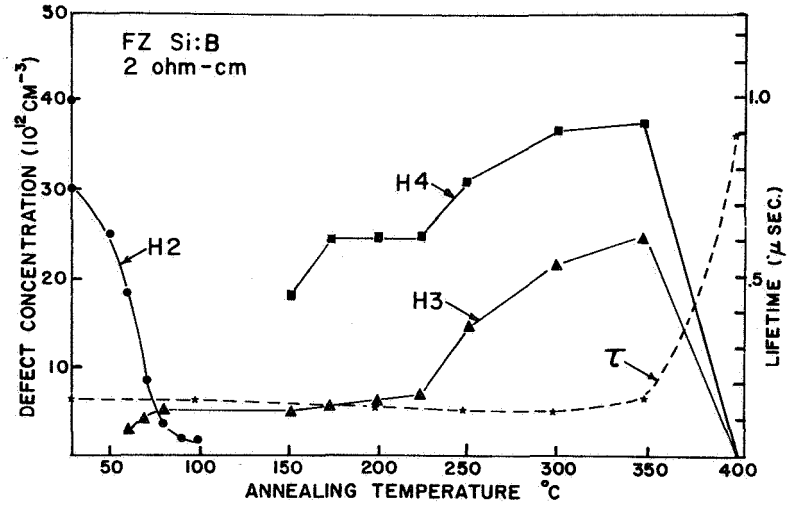

Figure 4. Isochronal anneal of 1-MeV electron irradiated ($5x10^{15}$ e/cm^2) 2-ohm-cm, boron-doped silicon showing behavior of three peaks (H2, H3, and H4) and recovery of lifetime.

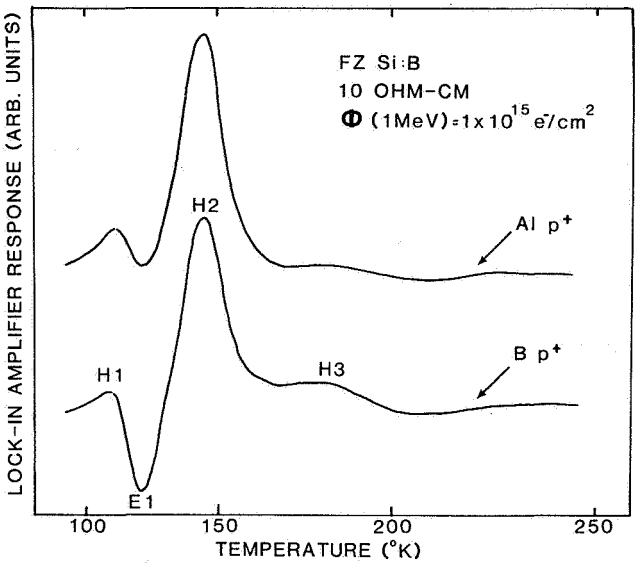

Figure 5. Comparison of DLTS spectra of electron-irradiated Al p^+ and B p^+ back surface samples from n^+-p-p^+ cells.

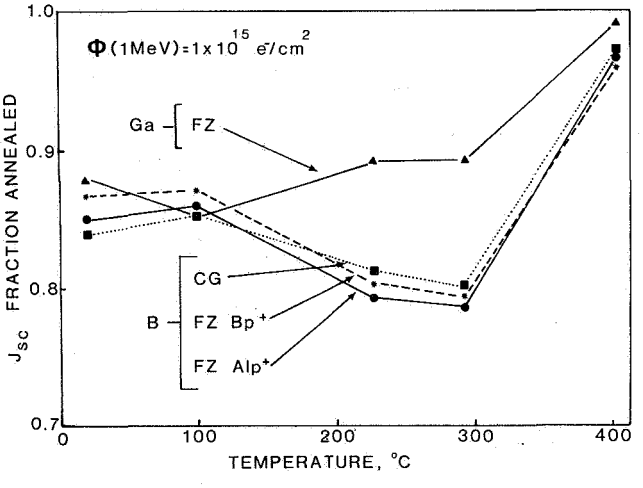

Figure 6. Isochronal anneal of short circuit current (J_{SC}) in electron-irradiated, silicon solar cells. Crucible-grown cell is 2 ohm-cm. All other cells are 10 ohm-cm.

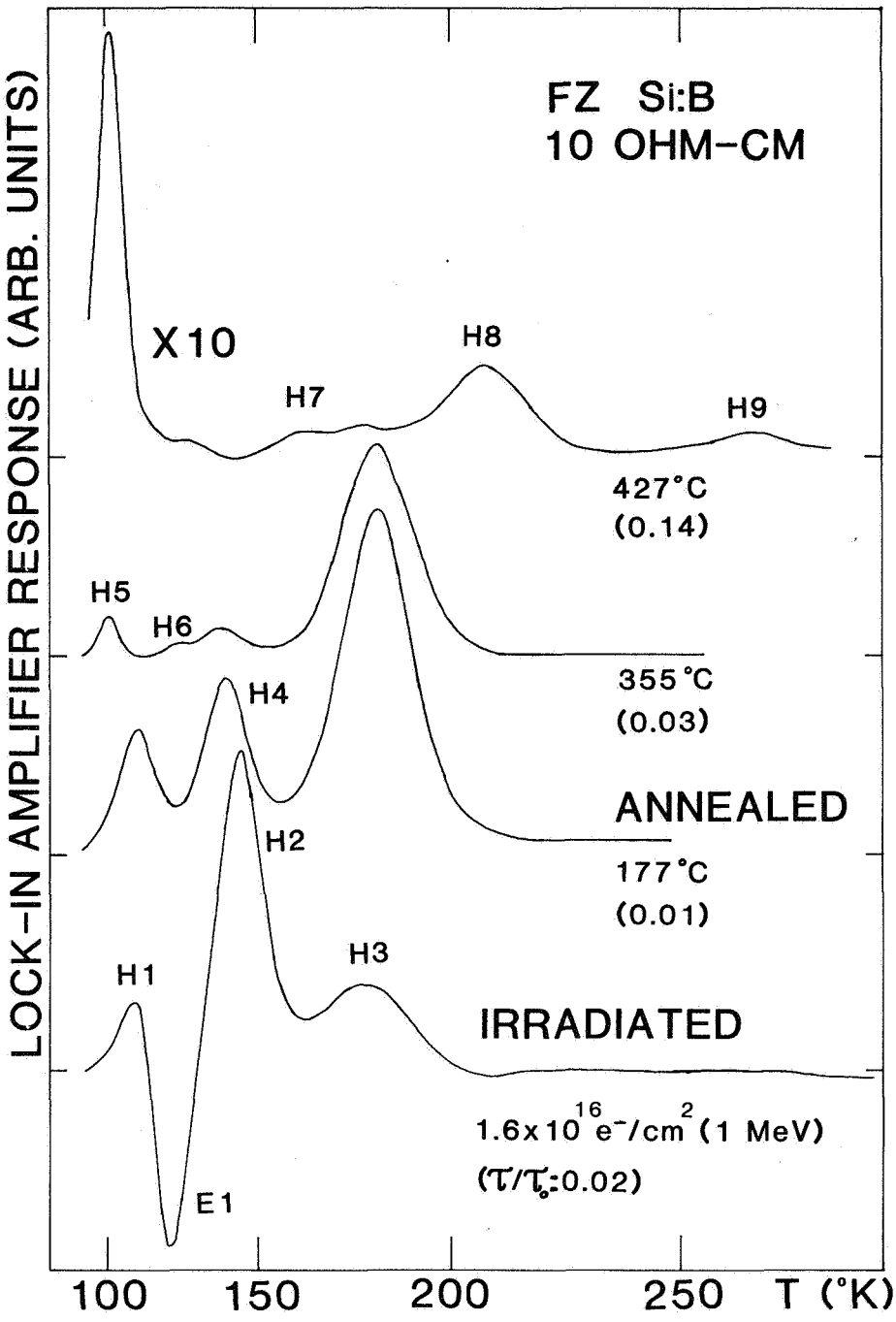

Figure 7. Typical DLTS spectra of boron-doped, B p^+ silicon cells after electron irradiation and several annealing steps. The fractional pre-irradiation lifetime is given in parenthesis.

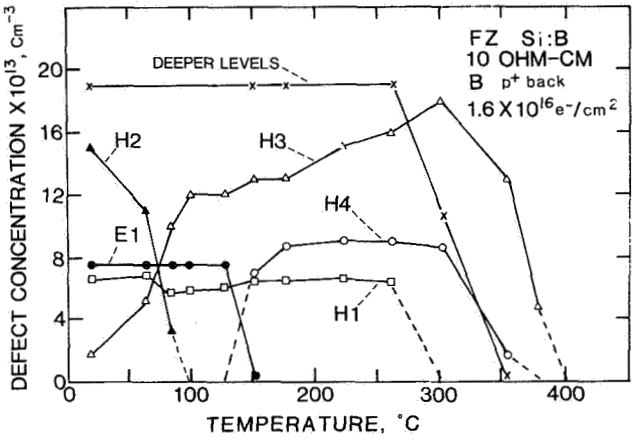

Figure 8. Isochronal anneal of principal defects and of deeper levels in electron-irradiated, boron-doped silicon.